

Magnetic Fluctuations at a Field-Induced Quantum Phase Transition

O. Stockert,¹ M. Enderle,² and H. v. Löhneysen³

¹Max-Planck-Institut für Chemische Physik fester Stoffe, D-01187 Dresden, Germany

²Institut Laue-Langevin, F-38042 Grenoble, France

³Physikalisches Institut, Universität Karlsruhe, D-76128 Karlsruhe, Germany, and Forschungszentrum Karlsruhe, Institut für Festkörperphysik, D-76021 Karlsruhe, Germany

(Received 9 December 2005; published 6 December 2007)

We report an inelastic neutron-scattering study at the field-induced magnetic quantum phase transition of $\text{CeCu}_{5.8}\text{Au}_{0.2}$. The data can be described better by the spin-density-wave scenario than by a local quantum critical point, while the latter scenario was shown to be applicable to the zero-field concentration-tuned quantum phase transition in $\text{CeCu}_{6-x}\text{Au}_x$ for $x = 0.1$. This constitutes direct microscopic evidence for a difference in the quantum fluctuation spectra at a magnetic quantum critical point driven by different tuning parameters.

DOI: 10.1103/PhysRevLett.99.237203

PACS numbers: 75.30.Mb, 71.27.+a, 75.20.Hr

Magnetic quantum phase transitions involving itinerant fermionic degrees of freedom have experienced a surge of recent interest. Here, as a function of some control parameter δ such as external pressure, chemical composition, or magnetic field, magnetic order can be suppressed and the system may undergo a zero-temperature transition from a magnetically ordered to a paramagnetic state at a critical value δ_c of the control parameter [1,2]. The standard model of a second-order magnetic quantum phase transition, according to Hertz, Millis, Moriya, and others [3–5], invokes scattering of electronic quasiparticles by incipient magnetic fluctuations. Thus, the quasiparticles acquire, for a three-dimensional (3D) ferromagnet, a logarithmically diverging mass with decreasing temperature T , leading to a logarithmically diverging Sommerfeld constant $\gamma = C/T$ of the specific heat C . On the other hand, for a 3D antiferromagnet, $\gamma \propto 1 - a'\sqrt{T}$ is expected, i.e., no divergence of γ for $T \rightarrow 0$, because critical scattering is confined to so-called “hot spots” on the Fermi surface connected by the ordering wave vector \mathbf{Q}_{AF} of the antiferromagnetic order [6,7].

Heavy-fermion systems are particularly well suited to investigate magnetic quantum phase transitions [2]. For instance, $\text{CeCu}_{6-x}\text{Au}_x$ is a system where with increasing Au concentration x incommensurate antiferromagnetic order develops out of a nonmagnetic ground state of CeCu_6 [8,9]. This nonmagnetic ground state is due to the strong hybridization between $4f$ -derived magnetic moments and conduction electrons. The system $\text{CeCu}_{6-x}\text{Au}_x$ has taken center stage because of a thorough investigation of thermodynamic and transport properties at the quantum critical point (QCP) obtained by concentration tuning at $x_c \approx 0.1$ [8,9], along with a detailed study of the critical magnetic fluctuations [10–12]. These studies have shown that the behavior of $\text{CeCu}_{6-x}\text{Au}_x$ near the QCP differs strongly from the predictions [3–5] of the Hertz-Millis-Moriya (HMM) model. While the observation of a logarithmic divergence of C/T near the antiferromagnetic QCP can

in principle be explained in terms of the HMM model invoking quasi-2D critical fluctuations [13], the origin of this lowering of dimensionality out of 3D antiferromagnetic order is not understood. Furthermore, the dynamic susceptibility near the QCP as measured with inelastic neutron scattering is incompatible with the HMM model, which predicts $\chi^{-1}(\mathbf{Q}_{\text{AF}}, \omega, T) = a^{-1}(T^{3/2} - i b \omega)$ [14]. It can be cast in the form $\chi^{-1}(\mathbf{q}, \omega, T) = c^{-1}[\theta^\alpha(\mathbf{q}) + (T - i\omega)^\alpha]$ for momentum transfer $\hbar\mathbf{q}$ and energy transfer $E = \hbar\omega$ of the neutrons, with an anomalous scaling exponent $\alpha = 0.8$ [11,12]. This form of $\chi^{-1}(\mathbf{q}, \omega, T)$ implies that the fluctuations become critical in the time domain independent of \mathbf{q} , i.e., everywhere in the Brillouin zone, not just for the \mathbf{q} values at the quasi-2D critical fluctuations where $\theta(\mathbf{q}) \rightarrow 0$. These findings prompted a surge of models invoking a breakdown of the Kondo effect at the QCP [15,16]. More recently, the concept of local criticality, developed to explain the $\text{CeCu}_{6-x}\text{Au}_x$ data, was also applied to YbRh_2Si_2 which is a stoichiometric system close to a QCP, with an antiferromagnetic ordering temperature $T_N = 70$ mK, and which exhibits a wealth of unusual behavior [17–21]. In particular, field tuning of the QCP was employed to demonstrate a change of the Hall constant as a function of magnetic field, which in a single-band model was taken as evidence for a discontinuity of the Fermi volume as $T \rightarrow 0$ when the field is swept across the field-induced QCP [20]. However, up to now no neutron-scattering data are available for this system.

$\text{CeCu}_{6-x}\text{Au}_x$ for $x > x_c$ offers the opportunity to study a field-induced QCP including inelastic neutron scattering. In particular, $\text{CeCu}_{5.8}\text{Au}_{0.2}$, which orders antiferromagnetically with a propagation vector $\mathbf{Q}_{\text{AF}} = (0.625, 0, 0.275)$ below $T_N = 250$ mK, is well suited for such a study, since already a small magnetic field of $B_c \approx 0.4$ T along the easy c axis suppresses the antiferromagnetic order [22]. Early specific-heat experiments on the related system $\text{CeCu}_{6-x}\text{Ag}_x$ [23] suggested that C can be described by the 3D HMM model. A detailed comparison

of pressure and magnetic field tuning in $\text{CeCu}_{5.8}\text{Au}_{0.2}$ investigated by specific heat and resistivity [22] revealed a decisive difference: while the pressure-tuned QCP bears resemblance to the concentration-tuned QCP for $x = 0.1$, hence pointing to a quasi-2D fluctuation spectrum, the field-induced QCP, with the field applied parallel to the easy c direction, was more akin to the 3D HMM scenario. In view of this puzzling situation, neutron-scattering experiments are mandatory to directly probe the fluctuations near a field-induced QCP in order to unravel the role of the tuning parameter in QCP scenarios. A detailed theoretical discussion of field tuning a QCP in an antiferromagnet has been given very recently by Fischer and Rosch [24]. A magnetic field, besides acting as a tuning parameter, induces a precession of the magnetic moments, thus affecting the spin dynamics. In this Letter, we report on a first inelastic neutron-scattering study of a field-tuned QCP.

The $\text{CeCu}_{5.8}\text{Au}_{0.2}$ sample (dimensions $\sim 8 \times 8 \times 8 \text{ mm}^3$) for this study was cut from a large single crystal grown by the Czochralski technique in a tungsten crucible. The same sample was used previously to determine the magnetic structure with elastic neutron scattering [25], while other pieces of the same crystal served for the investigation of thermodynamic and transport properties [22]. The neutron-scattering experiments were carried out at the Institut Laue-Langevin Grenoble, on the cold triple-axis spectrometer IN12. The crystal was mounted with the orthorhombic b axis vertical, i.e., perpendicular to the a^*c^* scattering plane. A horizontal magnetic field up to 2.5 T could be applied in the scattering plane along the c axis. The measurements were performed at temperatures between $T = 60 \text{ mK}$ and 5 K with a fixed final neutron energy $E_f = 2.74 \text{ meV}$ ($k_f = 1.15 \text{ \AA}^{-1}$) resulting in an energy resolution of $\sim 60 \mu\text{eV}$ (FWHM) at zero energy transfer. Due to the experimental setup, mainly limited by the access windows of the magnet, the measurements were restricted to $\mathbf{Q} \approx (1.38, 0, 1.74)$, the position of a magnetic satellite of the (202) nuclear reflection.

The inset of Fig. 1 displays, as an introduction to the system, the linear dependence of the Néel temperature in $\text{CeCu}_{6-x}\text{Au}_x$ on the Au concentration x for $x \leq 0.5$. For $\text{CeCu}_{5.8}\text{Au}_{0.2}$ with $T_N \approx 250 \text{ mK}$ the incommensurate antiferromagnetic order is manifested in magnetic Bragg reflections below T_N , as can be seen in Fig. 1 in elastic neutron-scattering scans across $\mathbf{Q} = (1.38, 0, 1.74)$ at zero magnetic field. Figure 2 shows the temperature and magnetic field dependence of the (1.38 0 1.74) magnetic Bragg reflection when the magnetic field is applied along the c direction. At zero magnetic field the intensity is seen to vanish at $T \approx 220 \text{ mK}$ in accordance with earlier neutron-scattering data and in fair agreement with thermodynamic measurements [25]. As expected, the long-range nature of the antiferromagnetic order breaks up at T_N , as indicated by the increase of the linewidth $\Delta\Omega$ above 210 mK. The situation in a magnetic field at lowest temperature $T = 60 \text{ mK}$ is slightly different [cf. Figs. 2(c) and 2(d)]. While

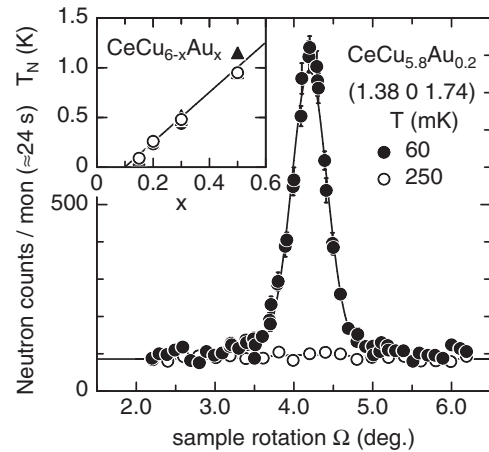


FIG. 1. Elastic neutron-scattering scans (rocking scans) across the position of a magnetic superstructure reflection at $\mathbf{Q} \approx (1.38, 0, 1.74)$ in $\text{CeCu}_{5.8}\text{Au}_{0.2}$ for different temperatures T_N of $\text{CeCu}_{6-x}\text{Au}_x$ as a function of Au concentration x for $x \leq 0.5$ determined by specific heat (triangles) and magnetic susceptibility (circles) [31]. In the inset, results on single crystals are marked by open symbols while closed symbols represent polycrystal measurements.

the linewidth of the magnetic Bragg peak starts to broaden already above $B = 0.15 \text{ T}$, the intensity vanishes around $B_c = 0.35 \text{ T}$ in agreement with specific-heat and electrical-resistivity measurements. The application of a magnetic field in a doped system, as is the case for $\text{CeCu}_{5.8}\text{Au}_{0.2}$, can lead to a slightly varying magnetization due to locally different environments. This was indeed inferred from the strong dependence of the residual elec-

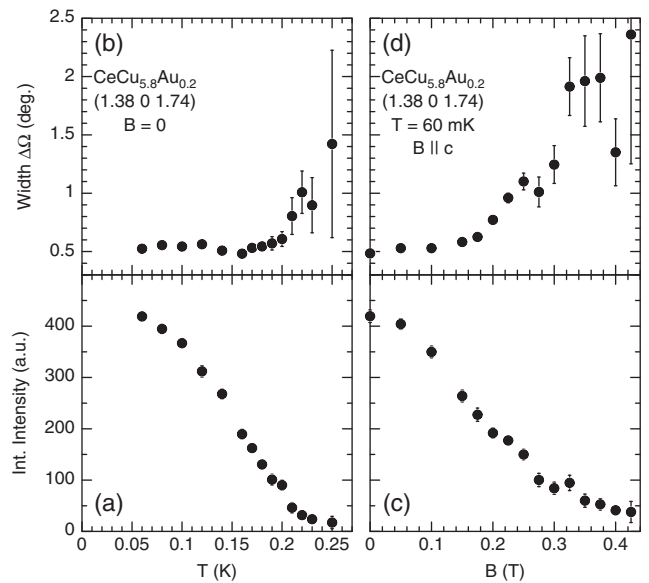


FIG. 2. Integrated intensity and linewidth (rocking width) of the (1.38 0 1.74) magnetic Bragg reflection in $\text{CeCu}_{5.8}\text{Au}_{0.2}$ as a function of temperature T in zero magnetic field (a), (b) and as a function of magnetic field applied along the c direction at $T = 60 \text{ mK}$ (c), (d).

trical resistivity as a function of pressure in the antiferromagnetically ordered state of CeCu_5Au [26]. Hence, magnetic domains might already form well below B_c , resulting in the observed broadening of the linewidth. Starting from long-range order the correlation length ξ decreases to $\xi \approx 70 \text{ \AA}$ at $T = 60 \text{ mK}$, $B = 0.3 \text{ T}$.

To investigate the critical spin dynamics at B_c scans were performed as a function of neutron energy transfer at the antiferromagnetic satellite position $\mathbf{Q} = (1.38, 0, 1.74)$ and at a magnetic field of $B = 0.35 \text{ T}$. Figure 3 shows energy scans at different temperatures. The data can be described by the sum of an incoherent elastic contribution (dotted lines in Fig. 3) and the quasielastic magnetic response with Lorentzian line shape (convoluted with the resolution, dashed lines in Fig. 3). To reliably perform the convolution and determine the shape of the incoherent signal the instrumental resolution has been measured on a vanadium sample and is best modeled by the sum of two lines with Gaussian line shapes (cf. inset of Fig. 3). The fits of the magnetic response yield a Lorentzian linewidth Γ strongly increasing with temperature, i.e., from a value well below the energy resolution of $\sim 60 \mu\text{eV}$ at $T = 60 \text{ mK}$ to $\Gamma = 0.68 \pm 0.21 \text{ meV}$ (FWHM) for $T = 5 \text{ K}$. Such a critical slowing down of

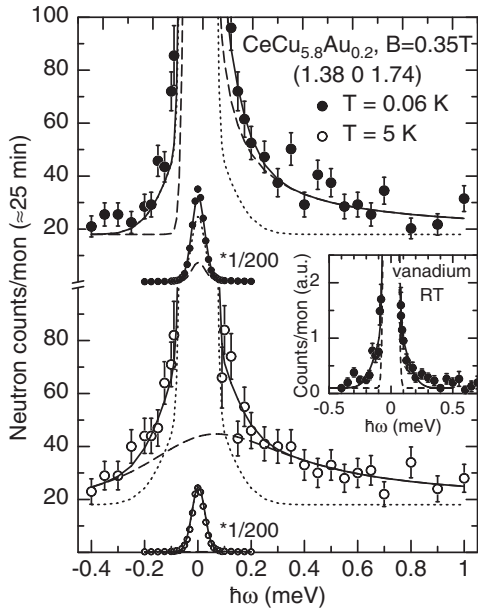


FIG. 3. Neutron-scattering intensity in $\text{CeCu}_{5.8}\text{Au}_{0.2}$ as a function of energy transfer $\hbar\omega$ at $\mathbf{Q} = (1.38, 0, 1.74)$ and $B = 0.35 \text{ T}$, $B \parallel c$ for $T = 60 \text{ mK}$ and 5 K . Solid lines represent fits to the data comprised of the incoherent elastic signal (dotted lines) and the quasielastic magnetic response with Lorentzian line shape convoluted with the resolution (dashed lines). The inset shows the tails of the energy resolution of the spectrometer as measured on vanadium at room temperature (RT), where the data have been normalized to 100 for the elastic peak value. The resolution, especially the tails, cannot satisfactorily be described by a function with a single Gaussian line (dashed line) but by a sum of two Gaussians (solid line).

the magnetic response as a function of temperature is expected at a QCP. Within the scatter of the data points, the Lorentzian fits work quite well. However, an anomalous susceptibility function $\chi(\mathbf{q}, \omega, T) = c\{[\theta^\alpha(\mathbf{q}) + [T - i\omega]^\alpha]^{-1}$, as found for $\text{CeCu}_{5.9}\text{Au}_{0.1}$ at zero field [11,12], would fit the data almost equally well.

Therefore, we finally present in Fig. 4 scaling plots of the imaginary part of the susceptibility χ'' in the form $\chi'' \cdot T^\alpha = f(\omega/T^\beta)$ for different neutron energy transfers $\hbar\omega$ and temperatures T as taken from data of Fig. 3 and additional scans. Here the data are plotted for (a) $\alpha = 0.8$, $\beta = 1$ and (b) $\alpha = 1.5$, $\beta = 1.5$. The susceptibility χ'' was obtained by $\chi'' = I[1 - \exp(-\hbar\omega/k_B T)]$, where I represents the neutron-scattering intensity after background subtraction. In the case of the locally critical scenario the scaling function $f(x)$ should read $f(x) = \frac{c \sin[\alpha \arctan(x)]}{(x^2 + 1)^{\alpha/2}}$ [11,12], while for the HMM scenario one expects $f(x) = \frac{abx}{1 + (bx)^2}$ [14]. Included in the plots are fits (solid lines) of the dynamical susceptibility to these scaling functions using a logarithmic weighing scheme (effectively the logarithm of χ'' was fitted). The ω/T scaling with the anomalous ex-

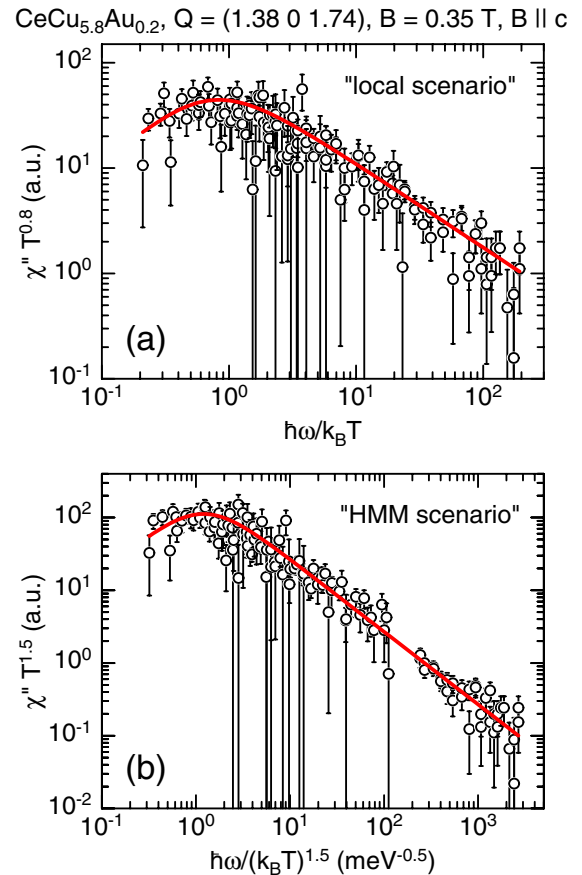


FIG. 4 (color online). Scaling plots of the imaginary part of the dynamic susceptibility $\chi''(\omega, T)$ at $\mathbf{Q} = (1.38, 0, 1.74)$, $B = 0.35 \text{ T}$, ($B \parallel c$) in $\text{CeCu}_{5.8}\text{Au}_{0.2}$ plotted as $\chi'' T^\alpha = f(\omega/T^\beta)$ with (a) $\alpha = 0.8$, $\beta = 1.0$ and (b) $\alpha = 1.5$, $\beta = 1.5$. Solid lines represent fits to the data. For details see text.

ponent $\alpha = 0.8$, discovered by Schröder *et al.*, for $\text{CeCu}_{5.9}\text{Au}_{0.1}$ at zero field [11,12], clearly yields for the present case of a field-induced QCP an inferior collapse of the data onto one curve, as compared to the conventional HMM scenario. The better collapse of the data within the HMM scenario is corroborated by a considerably higher correlation coefficient $R^2 = 0.960$ being much closer to the ideal value of 1 than $R^2 = 0.865$ in the locally critical scenario.

Our result has important implications. First, it suggests that the field-tuned QCP in $\text{CeCu}_{5.8}\text{Au}_{0.2}$ is driven by spin fluctuations at incipient spin-density-wave magnetic order. This is to be contrasted with the interpretation of a Fermi volume change at the field-induced QCP in YbRh_2Si_2 , which is based on Hall-effect data [20]. Lacking inelastic neutron-scattering data for this compound, there is a clear need for Hall-effect experiments for $\text{CeCu}_{5.8}\text{Au}_{0.2}$ across the field-induced QCP, which are underway to clarify this important point. Second, focusing on $\text{CeCu}_{6-x}\text{Au}_x$, the decisive difference between our present results for field tuning and earlier concentration-tuned data for inelastic neutron scattering, which is strongly backed by corresponding differences in thermodynamic and transport properties [9,22], points to a certain degree of “nonuniversality” of a QCP in a given system. In particular, the fact that pressure tuning of the QCP for samples with $x = 0.2$ and $x = 0.3$ yields the same temperature dependencies of the resistivity and specific heat at their respective critical pressures p_c [9] as the sample at the critical concentration $x = 0.1$ and $p = 0$, viz. $\Delta\rho \sim T$ and $C \sim -\ln(T/T_0)$, suggests that concentration and pressure tuning lead to similar critical fluctuations.

A speculative explanation of why $\text{CeCu}_{5.8}\text{Au}_{0.2}$ in a field parallel to the easy direction leads toward a QCP with a 3D fluctuation spectrum may be found in the strong magnetic anisotropy of the system. In $\text{CeCu}_{6-x}\text{Au}_x$, the ratio of the uniform static magnetic susceptibility at low temperatures is $\chi_c:\chi_a:\chi_b = 10:2:1$ for fields applied parallel to the principal axes (we use the orthorhombic notation for $\text{CeCu}_{6-x}\text{Au}_x$, ignoring the small monoclinic distortion for $x < 0.14$ [27]). This strong anisotropy also results in an extended field range where the antiferromagnetic phase is stable in CeCu_5Au for $B \parallel c$, where a spin-flop phase exists only for $2.3 \text{ T} \leq B \leq 3 \text{ T}$ [28]. At the bicritical point where antiferromagnetic, spin-flop, and paramagnetic phases meet, the system is in fact isotropic in spin space [29]. Even complex magnetic structures with additional chiral symmetry breaking exhibit (chiral) Heisenberg behavior at the corresponding tetracritical point [30]. Whether this idea is applicable to the field-induced QCP in $\text{CeCu}_{5.8}\text{Au}_{0.2}$ can be tested by a detailed study of the field-tuned QCP across the $\text{CeCu}_{6-x}\text{Au}_x$ series for different x . One should note that the locally critical scenario requires that the fluctuations of the incipient magnetic order are 2D. In this sense, there is a “consistency” that 3D behavior is restored once the system is

driven to the more conventional HMM scenario by a magnetic field.

In conclusion, we have presented inelastic neutron-scattering data demonstrating that the field-tuned quantum critical point in $\text{CeCu}_{5.8}\text{Au}_{0.2}$ presents a critical fluctuation spectrum distinctly different from that at the concentration-tuned quantum critical point in $\text{CeCu}_{5.9}\text{Au}_{0.1}$ at zero magnetic field. These data highlight the dual role of magnetic field and shed new light on the issue of local vs spin-density-wave scenario at the critical point as well as the role of dimensionality at magnetic quantum critical points.

We thank A. Rosch and Q. Si for helpful discussions. The help of J.L. Ragazzoni concerning the cryogenics is greatly acknowledged. This work was supported by the Deutsche Forschungsgemeinschaft within Contract No. LO 250/17-3 and by the Helmholtz Association of Research Centers via VH-VI-127.

-
- [1] S. Sachdev, *Quantum Phase Transitions* (Cambridge University Press, Cambridge, 1999).
 - [2] G. Stewart, *Rev. Mod. Phys.* **73**, 797 (2001).
 - [3] J. Hertz, *Phys. Rev. B* **14**, 1165 (1976).
 - [4] A.J. Millis, *Phys. Rev. B* **48**, 7183 (1993).
 - [5] T. Moriya and T. Takimoto, *J. Phys. Soc. Jpn.* **64**, 960 (1995).
 - [6] R. Hlubina and T.M. Rice, *Phys. Rev. B* **51**, 9253 (1995).
 - [7] A. Rosch, *Phys. Rev. B* **62**, 4945 (2000).
 - [8] H.v. Löhneysen *et al.*, *Phys. Rev. Lett.* **72**, 3262 (1994).
 - [9] H.v. Löhneysen, *J. Phys. Condens. Matter* **8**, 9689 (1996).
 - [10] O. Stockert *et al.*, *Phys. Rev. Lett.* **80**, 5627 (1998).
 - [11] A. Schröder *et al.*, *Phys. Rev. Lett.* **80**, 5623 (1998).
 - [12] A. Schröder *et al.*, *Nature (London)* **407**, 351 (2000).
 - [13] A. Rosch *et al.*, *Phys. Rev. Lett.* **79**, 159 (1997).
 - [14] Q. Si (private communication).
 - [15] P. Coleman *et al.*, *J. Phys. Condens. Matter* **13**, R723 (2001).
 - [16] Q. Si *et al.*, *Nature (London)* **413**, 804 (2001).
 - [17] O. Trovarelli *et al.*, *Phys. Rev. Lett.* **85**, 626 (2000).
 - [18] P. Gegenwart *et al.*, *Phys. Rev. Lett.* **89**, 056402 (2002).
 - [19] J. Custers *et al.*, *Nature (London)* **424**, 524 (2003).
 - [20] S. Paschen *et al.*, *Nature (London)* **432**, 881 (2004).
 - [21] P. Gegenwart *et al.*, *Phys. Rev. Lett.* **94**, 076402 (2005).
 - [22] H.v. Löhneysen *et al.*, *Phys. Rev. B* **63**, 134411 (2001).
 - [23] K. Heuser *et al.*, *Phys. Rev. B* **57**, R4198 (1998); **58**, R15959 (1998).
 - [24] I. Fischer and A. Rosch, *Phys. Rev. B* **71**, 184429 (2005).
 - [25] H.v. Löhneysen *et al.*, *Eur. Phys. J. B* **5**, 447 (1998).
 - [26] H. Wilhelm *et al.*, *J. Phys. Condens. Matter* **13**, L329 (2001).
 - [27] K. Grube *et al.*, *Phys. Rev. B* **60**, 11 947 (1999).
 - [28] C. Paschke *et al.*, *J. Low Temp. Phys.* **97**, 229 (1994).
 - [29] W. Gebhard and U. Krey, *Phasenübergänge und kritische Phänomene* (Vieweg, Braunschweig, 1980), p. 98.
 - [30] D. Beckmann *et al.*, *Phys. Rev. Lett.* **71**, 2829 (1993).
 - [31] T. Pietrus *et al.*, *Physica B (Amsterdam)* **206–207**, 317 (1995).